OFFICE OF NAVAL RESEARCH

Contract N00014-89-J-1103

R & T Code: 413e022

Technical Report No. 49

SPECTROSCOPIC EVIDENCE FOR CARBON-CARBON BONDING IN CARBIDE LAYERS ON METALS

By

F.L. Hutson, D.E. Ramaker, and B.E. Koel

Prepared for Publication

In

Surface Science

GEORGE WASHINGTON UNIVERSITY
Department of Chemistry
Washington, D.C. 20052

December, 1989

SECURITY CLASSIFICATION OF THIS PAGE

REPORT DOCUMENTATION PAGE

1a. REPORT SECURITY CLASSIFICATION: Unclassified	1b. RESTRICTIVE MARKINGS
2a. SECURITY CLASSIFICATION AUTHORITY	3. DISTRIBUTION/AVAILABILITY OF REPORT: Approved for public release; distribution unlimited
2b. DECLASSIFICATION/DOWNGRADING SCHEDULE	
4. PERFORMING ORGANIZATION REPORT NUMBER(S): Technical Report #49	5. MONITORING ORGANIZATION REPORT NUMBER(S)
6a. NAME OF PERFORMING ORGANIZATION: Dept. of Chemistry, George Washington Univ. / 6b. OFFICE SYMBOL (If applicable)	7a. NAME OF MONITORING ORGANIZATION: Office of Naval Research (Code 418)
6c. ADDRESS (City, State, and ZIP Code): Washington, DC 20052	7b. ADDRESS (City, State, and ZIP Code): Chemistry Program, 800 N. Quincy Street, Arlington, VA 22217
8a. NAME OF FUNDING/SPONSORING ORGANIZATION: Office of Naval Research / 8b. OFFICE SYMBOL (If applicable)	9. PROCUREMENT INSTRUMENT IDENTIFICATION NUMBER: Contract N00014-89-J-1103
8c. ADDRESS (City, State, and ZIP Code): Chemistry Program, 800 Nth, Quincy, Arlington, VA 22217	10. SOURCE OF FUNDING NUMBERS: PROGRAM ELEMENT NO. / PROJECT NO. / TASK NO. R & T 413e022 / WORK UNIT ACCESSION NO.

11. TITLE (Include Security Classification): Spectroscopic Evidence for Carbon-Carbon Bonding in Carbide Layers on Metals (unclassified).

12. PERSONAL AUTHOR(S): F.L. Hutson, D.E. Ramaker and B.E. Koel

13a. TYPE OF REPORT	13b. TIME COVERED	14. DATE OF REPORT (Year, Month, Day)	15. PAGE COUNT
Interim Technical	FROM ____ TO ____	December 1989	42

16. SUPPLEMENTARY NOTATION: Prepared for publication in Surface Science

17. COSATI CODES			18. SUBJECT TERMS (Continue on reverse if necessary and identify by block number)
FIELD	GROUP	SUB-GROUP	Carbides, graphite, Auger Spectroscopy, EELS, Photoemission

19. ABSTRACT (Continue on reverse if necessary and identify by block number)

We examine previously reported ultraviolet photoelectron, C K electron energy loss, and C KVV Auger spectroscopic data from carbidic layers formed at temperatures between 500-650K on Ni(100), Ru(001), and other metals. These data indicate that significant amounts of carbon-carbon bonding, such as that from C_2^n, C_3^n etc. fragments, exists on the surface in addition to the carbon-metal bonding with the substrate. The carbidic layers can be made from either CO or $C_2H_4^n$ exposure to the metal surface.

Quantitative interpretation of the Auger data indicate that the carbon-carbon to carbon-metal bonding ratio lies between 0.3 and 0.5 . Observed changes in the spectra obtained from different surfaces or at different coverages are accounted for by variations in this ratio.

20. DISTRIBUTION/AVAILABILITY OF ABSTRACT	21. ABSTRACT SECURITY CLASSIFICATION
☒ UNCLASSIFIED/UNLIMITED ☒ SAME AS RPT. ☐ DTIC USERS	Unclassified
22a. NAME OF RESPONSIBLE INDIVIDUAL: Dr. David L. Nelson	22b. TELEPHONE (Include Area Code): (202) 696-4410 / 22c. OFFICE SYMBOL

DD FORM 1473, 84 MAR — 83 APR edition may be used until exhausted. All other editions are obsolete.

SECURITY CLASSIFICATION OF THIS PAGE: Unclassified

SPECTROSCOPIC EVIDENCE FOR CARBON-CARBON BONDING IN "CARBIDIC" LAYERS ON METALS.

F.L. Hutson[a] and D.E. Ramaker[a]

Chemistry Department

George Washington University

Washington, DC 20052

and

B.E. Koel

Department of Chemistry and Biochemistry, and

Cooperative Institute for Research in Environmental Sciences (CIRES)

University of Colorado, Boulder, CO 80309

[a]Supported by the Office of Naval Research

Abstract

We examine previously reported ultraviolet photoelectron, C K electron energy loss, and C KVV Auger spectroscopic data from "carbidic" layers formed at temperatures between 500- 650K on Ni(100), Ru(001), and other metals. These data indicate that significant amounts of carbon-carbon bonding, such as that from C_2, C_3, etc. fragments, exists on the surface in addition to the carbon-metal bonding with the substrate. The carbidic layers can be made from either CO or C_2H_4 exposure to the metal surface. Quantitative interpretations of the Auger data indicate that the carbon-carbon to carbon-metal bonding ratio lies between 0.25 and 0.4. Observed changes in the spectra obtained from different surfaces or at difference coverages are accounted for by variations in this ratio.

1. Introduction

The interaction of ethylene and acetylene with single crystal metal surfaces has been studied for many years. From techniques such as high resolution electron energy loss spectroscopy (HREELS) [1-9], temperature programmed desorption (TPD) [6-14], and ultraviolet and x-ray photoelectron spectroscopy (UPS and XPS) [13-16], it has been possible to identify the mode of adsorption of these C_2 hydrocarbons and determine the paths for dehydrogenation at higher temperatures. Recently [6-26], emphasis has been placed on the carbonaceous layers which result at still higher temperatures, since these layers are known to be very similar to those involved in Fischer-Tropsch synthesis, which converts carbon monoxide and hydrogen into a mixture of hydrocarbons. The recent interest in the production of synthetic diamond has also motivated such studies [27]. In addition to those basic techniques mentioned above, recent work has also utilized electron energy loss spectroscopy (EELS) [15,17,18], surface extended energy loss fine structure (SEELFS) [19,28], secondary ion mass spectroscopy (SIMS) [6,10,11,20], near edge x-ray absorption fine structure (NEXAFS) [21], and Auger electron spectroscopy (AES) [17,18,22-25,29].

At least two, and possibly three, distinct carbonaceous states have been observed on transition metal surfaces [17,18,22-25]. A carbidic carbon, which is very active in the methanation and Fisher-Tropsch synthesis and exists at temperatures ranging from 450-600K, and a graphitic carbon, which poisons the catalytic metal surface above 650 K, have definitely been identified [22-25]. Evidence for an intermediate state on some metals between 570-670 K has been given, but little is known about it, and no structure has been proposed [17,18]. These states will be identified in the figures as the C, G, and I phases, respectively.

Although HREELS has been very powerful for elucidating the structure

of hydrocarbons on surfaces [1-9], it has not been real helpful for studying carbonaceous layers, since it cannot distinguish the various forms of carbon. SIMS has been very helpful in indicating the degree of mobility of the carbon atoms at different temperatures [19] and the presence or absence of hydrogen atoms, but, SIMS is not an in-situ study, so that one is never certain if the various fragments analyzed actually existed on the surface, or were formed in the "plasma" above the surface [6,10,11,20]. A recent SEELFS study [19] has been helpful in determining the structure of isolated C on Ni(100), but again it is not useful for identifying the different states.

Most helpful in identifying the three different phases or states has been the direct electron spectroscopies, AES, EELS, and UPS. In particular, AES has been most helpful in identifying the "carbidic" and "graphitic" forms of carbon [22-25], and indicating a distinct intermediate but unknown form around 570-670 K on Ni and Cu [17,18]. EELS has also suggested the presence of an intermediate form in this temperature range [17,18].

In this work we carefully examine and interpret previously reported UPS [14,15], ELS [17],and AES [23,24,29] data from carbonaceous layers on Ni(100), Ru(001) or other surfaces of Ni at different temperatures above 500K. The layers were made from either CO or C_2H_4 exposure to the metal surface, with little differences noted in the data or expected in this temperature region, provided similar carbon coverages are obtained. All spectra indicate significant amounts of C-C bonds (i.e. C_x x=2,3, etc.) exist below 670K. In fact, only 40-65 % of the "carbidic" Auger spectra, which are semi-quantitatively interpreted, actually arise exclusively from carbidic bonding (i.e. carbon-metal bonding). The intermediate carbonaceous state, in the temperature range 570-670 K, is shown to arise from a relative decrease in the C-C bonding character due to partial C-C bond cleavage, which apparently occurs on Ni(100) and Cu(100) at temperatures below that for the formation of

graphite. The differences seen in the published spectra for CO/metals at 650K are also attributed to differing amounts of C_x, as this obviously varies with carbon coverage, temperature, and surface treatment.

We believe this work to be the first to identify direct electron spectroscopic evidence for the existence of C_x in carbonaceous layers on metals. It is, however, consistent with the work of Lauderback and Delgass [10], who utilized isotopic $C^{13}{}_2H_4$ and $C^{12}{}_2H_4$ mixtures, and temperature programmed negative ion SIMS, which suggests that a preservation of close C-C distances for the two carbon atoms of the parent ethylene molecule exists up to 600K on Ru(001), followed by an enhanced carbon mobility above 600K. In contrast, White and co-workers [6,11] utilizing several techniques concluded that coadsorbed K and C_2H_4 on Pt(111), and coadsorbed CO and C_2H_4 on Ru(001) proceeded sequentially from CCH or C_xH to C_x to graphite, without complete C-C bond cleavage. This different behavior on Pt and Ru will be discussed in Sec. 6.

We acknowledge that it is difficult to distinguish C-H and C-C bonding from electron spectroscopic data since they have similar binding energies [16,30]. Therefore, we cannot rule out some C-H bonding character at the surface. This is particularly true since all of the spectroscopic data are obtained at room temperature after flashing to the indicated higher temperatures [14,15,17,23,24]. At room temperature the highly active carbon could rehydrogenate before the data taking is completed. However, experimental evidence argues against this. Little evidence has been seen for changes in the spectroscopic data with time [14]. Furthermore, SIMS and TPD data indicate the near lack of hydrogenated carbon species coming off the surface after flashing to temperatures above 500K [6,10-12,20]. This indicates that rehydrogenation is not important under most experimental ultrahigh vacuum conditions, and that C-H bonding character is nearly absent on the surface after flashing.

The ability to distinguish C-C vs. C-M bonding character arises because these two bonds, in contrast, are very different in binding energy, as we will see below. This primarily arises because the C-C bond has a much stronger bonding energy compared with the C-M bond. In gas phase hydrocarbons, the C-C and C-H bonds are so similar in character, that delocalized molecular orbitals are formed, which are characterized by the global symmetry of the molecule. However, at the metal surface, the C-C and C-M bonds are so different in binding energy that some MO's are localized primarily on the C_x adsorbate, and others on the C-M adsorbate-substrate bonds. Thus the electron spectroscopic lineshapes should have spectral regions which reflect the C-C bonds (and C-H bonds if present), and those which reflect the C-M bonds, making it possible to determine the extent of each.

Sections 2, 3, and 4 summarize our interpretation of previously reported UPS, ELS, and AES data, respectively. A brief summary and conclusions are given in Sec. 6.

2. Interpretation of UPS data

Figure 1 compares estimates of the C valence band density of states (DOS) for a carbonaceous layer on different metals. Rosei et al [15] obtained UPS data for carbidic overlayers obtained by heating a Ni (111) surface at about 500 K in CO. The difference between the UPS ($h\nu$ = 35 eV) spectra for the clean and carburized Ni surface, as given in Fig. 1, represent an estimate of the DOS on the C atoms. Koel et al [14] obtained UPS data for carbidic overlayers obtained by saturation exposure (0.38 ML) to C_2H_4 of a Ni(100) surface at 100 K and subsequent warm-up to 580K. The difference between the UPS (He II) spectra for the clean and exposed surface without any scaling of the intensities is also indicated in Fig. 1.

Since the data is expected to vary with carbon coverage, care is taken

to indicate this throughout, but these estimates are often very crude. Rosei et al [15] estimate their carbon coverage at 0.3 ML; Koel et al [14] estimate a coverage of 0.38 ML. On Ni(100), one-half of this is believed to desorb below 580K, the temperature at which the carbidic carbon appears [12]. This gives a carbidic coverage of just 0.19 ML on Ni(100). The carbidic coverage on Rosei's Ni(111) surface is not known.

The difference spectra in Fig. 1 are compared with the LCAO-MO calculated DOS obtained by Feibelman [31] for a (1x1) overlayer of C atoms on an 11-layer Ru(0001) film, with only 1/3 of the three-fold sites filled with carbon atoms. In this theoretical model, the carbon atoms are relatively isolated since the nearest C-C distance is greater than 5.0 a.u. compared with a C-C distance of 2.68 a.u. in graphite [31]. Thus we assume that the theoretical DOS is indeed representative of only C-M bonding.

The calculated results indicate that the narrow feature near the Fermi level in both the empirical and calculated "DOS" is due predominantly to a non-bonding p_z orbital. The broad feature between 2 and 8 eV arises primarily from the bonding p_{xy} orbitals, and the feature from 11 to 15 eV arises mainly from the s orbitals [31]. This DOS can be qualitatively understood as arising from C atoms tetrahedrally sp^3 bonded with its three neighboring substrate atoms, leaving a non-bonding, dangling p_z band partially filled. Feibelman attributes the activity of the carbidic carbon to the partially filled p_z band, and the inactivity of the graphitic layer which forms at higher coverages to the π bonding between the p_z orbitals [31].

General agreement between the three curves in Fig. 1 is found, but significant differences are noted. First, all three curves exhibit the p_z feature near the Fermi level, but they are significantly different in size. This is to be expected, considering that the metal DOS is very large near the Fermi level, so that the difference spectra are very sensitive to the subtraction procedure, and reflect the change in the metal DOS as well (i.e. the difference curves actually go negative right at the Fermi level because of shifts in the metal 3d DOS) [14,15]. We also believe that the feature at 1.5 eV in the Koel data is not due entirely to the p_z contribution, but arises primarily from the p_{xy} DOS, so that the p_z contribution appears as the slight shoulder around 1 eV.

The agreement between the Rosei data and the Feibelman results for the p_{xy} feature is remarkable, both containing roughly the same structure. The Koel data reveals two large p_{xy} peaks roughly similar to the Feibelman data, but shifted by about 2 eV to the Fermi level. This is particularly true if we identify the feature around 1.5 eV in the Koel data with the p_{xy} contribution as indicated above.

The reason for this shift of the p_{xy} feature in the Koel data is not clear. Calculations by Joyner et al [25] indicate that the p_{xy} feature moves slightly toward the Fermi level as the carbon-metal bond energy decreases, and we expect the Ru-C bond to be stronger than the Ni-C bond. However, the Rosei data for a Ni(111) surface, and Feibelman's calculations for a Ru(0001) surface have the p_{xy} features aligned very nicely. Perhaps the different Ni(100) vs the Ni(111) surfaces are responsible for the differences in the Rosei and Koel data. It is well known for example, that upon saturation exposure to ethylene at 100K in an ultra-high vacuum, carbidic carbon changes to graphitic carbon on Ni(111) around 600K, but not the on Ni(100) surface [23]. LEED results also indicate that the Ni(100) surface reconstructs upon exposure to C, in contrast to the Ni(111) surface [32]. All of this may indicate that the Ni-C bond energy is smaller on the Ni(100) surface, than on the Ni(111), resulting in the shift to lower binding energy for the Ni(100) surface. In any event, the Auger data for C/Ni(100), to be discussed below, also indicate that indeed, the p_{xy} feature has a smaller binding energy than

that indicated by Feibelman for C/Ru.

The "s" feature is sharp and around 11 eV in the calculated DOS, very broad and centered at 15 eV in the Rosei data, and centered around 12 eV in the Koel data. The slow tailing off of the empirical "s" feature in the Rosei data may be an artifact of the subtraction procedure. Perhaps the maximum at 13 eV in the Rosei data more correctly determines the position of the s DOS, which gives better agreement with the other two curves.

Most significant in this work, is the feature around 8.5 eV in the Koel data. We believe this feature arises from C-C bonding. For ethylene on Ni(100), the σ_{C-C} bond orbital feature has been previously [14] identified at 8.4 eV, and it still remains at 580 K when all hydrogen has desorbed. This feature is completely absent in Feibelman's theoretical results in Fig. 1, as expected in the absence of C-C bonding. It is also essentially absent in the Rosei data; we believe because the carbidic carbon coverage is significantly less than the 0.3 ML as estimated by Rosei, and because he started with CO/Ni so that much less C-C bonding is expected. We will see below that the EELS data also indicates less C-C bonding in the Rosei data, than on the Ni(100) surface.

3. Interpretation of K edge EELS data

Fig. 2 compares the $d^2N(E)/dE^2$ K edge EELS curves for four different carbonaceous layers on metals [15,17]. Curve "a" is for a graphitic carbon layer on Ni(110) (since a graphitic layer does not easily form on Ni(100) in UHV, we show the results for Ni(110) here), curve "b" for a so called carbidic layer on Ni(100), curve "c" for an "intermediate" layer on Ni(100) at 620 K, and curve "d" for a 0.3 ML "carbidic" layer on Ni(111). Curves a-c were reported by Caputi et al [17], who prepared the carbon layers by exposure of the metal surfaces to CO at a pressure of 1×10^{-5} for 30 Min at 520 K, with subsequent heating to form the various carbon layers. Although Caputi et al do not estimate the C coverage, at these low CO pressures, the coverage is believed to be less than or equal to 1 ML. Curve "c" was reported by Rosei et al [15], and corresponds to the same coverage (probably significantly less than 0.3 ML) discussed above. The K binding energy is about 283 eV for graphite [34], and 283.6 eV for a carbidic layer on a transition metal [14].

The peaks at 285 eV and 292 eV are known to arise from 1s-π and 1s-σ excitations respectively in graphitic layers [15]. The 1s-π peak falls very near the Fermi level because of excitonic effects [15,34]. Although excitonic effects are not expected in metals, graphite is a semimetal (i.e. the DOS in graphite and apparently also in graphitic overlayers are very small). For the intermediate layers, no excitonic-like peak is expected because of the large p_z DOS near the Fermi level. A small shoulder right near the Fermi level on curve "c" is attributed to the 1s-p_z excitations, and the feature around 291 eV to 1s-$p_{x,y}$ (i.e. 1s-σ) excitations. Curve "b" however reveals a large feature near the Fermi level again suggesting an excitonic-like peak, with only a plateau at 292 eV. This is indeed consistent with a less metallic entity, which may arise from a substantial decrease of p_z orbital character near the Fermi level due to the C-C bonding which still exists at these lower temperatures. Consistent with the UPS data and the expected lower coverages, the data of Rosei (curve d) reveal attributes of both curves b and c, indicating significant amounts of both C and C_x on the surface. Notice, that curves b, c, and d all show a small feature at 304 eV, and the relative intensity, I(304)/I(291), stays very constant for all three curves. This suggests that the peak at 304 eV also arises from C_x excitation.

4. Interpretation of Auger data - Empirical

4.a The "bulk" carbide lineshapes

The transmission metal carbides, MC_x, have been studied often with AES.

Recently Shulga and Gutsev presented dN(E)/dE Auger spectra for a series of carbides in the first three rows of the transition metal series [35]. These spectra show a small high energy feature around 275 eV, the principal feature around 272, a doublet feature around 263, and a small feature at 253 eV. Pehrsson and Ramaker [36] reported a detailed interpretation of the TiC and NbC lineshapes, and Gruzalski et al of the TaC lineshape [37]. They identify the 253, 263, 272, and 275 eV features as arising predominantly from the ss, sp, pp, and pp components, respectively, of the DOS self-fold. Both the principal and high energy features arise from the pp component (this is sometimes separated into the $\sigma\sigma$ and $\sigma\pi$ components), the doublet at 263 arises because the sp component splits into ^1P and ^3P multiplets due to the spin interaction. The pp component is apparently unaffected by localization effects (i.e. the lineshape is not significantly distorted from the one-electron self-fold); but, the sp and ss do have some localization effects [36,37]. Pehrsson and Ramaker [36] have also correlated these effects with the heat of formation (ΔH) of the metal carbide, the highly stable carbides being more ionic, the unstable carbides being more metallic. Thus the ratio I(275)/I(272) decreases but the features become more distinct with increasing ΔH, the ^1P–^3P separation increases with ΔH, and the localization effects in the ss and sp contributions increase with ΔH. Finally the C 1s binding energy shift relative to graphite increases with ΔH [36].

Ni_3C is thermally an unstable carbide [26,38]. It is generally produced by the carburization of Ni films in CO around 550-650 K resulting in a "thin" film of Ni_3C rather than a true bulk carbide. Ni_3C has been studied previously by x-ray diffraction, LEED, TEM, AES, and XPS [38-42].

The AES lineshape of Ni_3C was first presented by Coad and Riviere [39]; higher resolution lineshapes have been presented by Chang [43] and Salmeron et al [44]. C KVV Auger lineshapes, N(E), for Ni_3C are presented in Fig. 3

(curves b and c). They were obtained from the data of Chang [43], and Salmeron et al [44], respectively. The two spectra have been placed on a two-hole binding energy scale by aligning the principal peak with that in the Koel data [24], curve f. No attempt was made to deconvolute out experimental broadening in these two curves, so that these two spectra are believed to be at much lower resolution than all of the others in Fig. 3. The two spectra are similar except for an apparent greater broadening of the Salmeron et al spectrum. This may be due to the resolution of their spectrometer.

The two "bulk" spectra in Fig. 2 are consistent with that expected for a relatively unstable carbide as indicated above. The shoulder at 15 eV is large but barely visible. The ^1P–^3P separation is not visible, and the C 1s binding energy is within 1 eV of that for graphite (i.e. about 283.6 eV for carbides [14] vs. 282.9 for graphite [34]). To be totally consistent within the above trends, no localization effects should be visible in any of the ss, sp or pp features. Thus a self-fold of the one-electron DOS with the appropriate atomic matrix elements and screening factors should closely reproduce the Auger spectra for Ni_3C.

4.b The surface carbidic lineshapes

Fig. 3 compares several Auger lineshapes that have been referred to in the literature as carbidic in character. The top lineshape (curve f) is that reported by Koel [24] upon heating of ethylene on Ni(100) to a temperature of 600 K. The second lineshape (curve e) is that observed by Houston et al [22,23] upon exposure of a Ni(100) surface to 24 Torr CO for 1000 sec at 600 K. The third lineshape (curve d also reported by Houston et al [23]) is that from a Ni(111) surface after electron beam cracking of CO. Catalytic or electron beam cracking of CO produces "carbidic" carbon on either Ni surface [22]. The coverages for the latter two have been roughly estimated to be about 0.1–0.2 ML, that for the Koel data at about 0.19 ML. The bottom curve,

curve a, is from the data of Caputi et al [17]. All of the data were obtained from the raw data after integration, subtraction of a linear background, and deconvolution of inelastic loss contributions. For the Caputi data, the loss contributions were subtracted by the Shirley method [45] so that instrumental broadening was not subtracted in this case, like it was for the Koel and Houston data. The Caputi and Koel data were placed on a two-hole binding energy scale by using a C 1s binding energy of 283.6 eV and a work function of 4.4 eV [14]. The Houston data was energy aligned with the Koel data.

Several observations can be made from Fig.3. The carbide and surface carbidic lineshapes all have the familiar ss, sp and pp features, but otherwise they are quite different. The so called ss and sp features in the carbidic lineshapes are much sharper and larger than in the carbide lineshapes. The high energy shoulder is also much more distinct in the carbidic lineshapes.

Within the surface carbidic lineshapes, surprising agreement exists between the data of Koel [24] and Houston et al [23] for the Ni(100) surface. Six similar features are seen at the same energies in both spectra, only the relative intensities are somewhat different. This is true in spite of the fact that the Koel data was generated by the fragmentation of C_2H_4, and the Houston data by CO. On the other hand, the Houston data for Ni(100) and Ni(111), both generated by the CO carburization of Ni, is very different. Indeed the data for the Ni(111) surface appears closer to the "bulk" data.

Houston et al [23] have suggested that the differences between the carbidic lineshapes on Ni (100) and (111) are due to the different sp^n hybridizations on a two- or three-fold bonding site. Hybridization effects are clearly evident in the lineshapes exhibited by gas phase methane, ethylene, and acetylene [46]. However, we have shown previously that the DOS self-folds for benzene and cyclohexane, for example, are surprising similar; only after the hole-hole localization effects are included do the lineshapes

significantly vary [46]. Thus, the hybridization effects seen in the gas phase spectra are not a DOS phenomena, rather they are a hole-hole repulsion phenomena. But, at the metal surface in the carbides, the hybridization effect should be turned off, because the hole-hole repulsions are turned off due to metallic screening.

In this work we will show, via a quantitative interpretation, (Sec. 5) that differing amounts of C-C and C-M bonding character can account for the observed differences between the surface carbidic lineshapes as well as between the surface and bulk lineshapes. That indeed both C-C and C-M bonding character actually exists in the Auger lineshapes is indicated just by examining the differences between the surface carbidic lineshapes reported by Caputi et al [17] at 500 and 620 K (i.e. the C and I phases).

Figure 4 compares the dN(E)/dE Auger data of Caputi et al [17] obtained at 500 and 620 K (curves a and b for the C and I phases). Consistent with the UPS and EELS data, these spectra should reflect both the presence of C-C and C-M bonding, the "intermediate" lineshape reflecting the presence of more C-M than the carbidic lineshape. If we assume this is true, then an appropriate difference of the two spectra should reflect pure C-M bonding. We show various difference spectra, [I- xC] in Fig. 4, where "x" is a weighting factor between the two curves when the peak-to-peak height is normalized equally. The difference curves and the full spectrum have similar structural features, but the difference curves are shifted to lower binding energy by about 2 eV. Figure 5 compares N(E) data for the "carbidic" 500K spectrum and for the difference curves. The I - xC difference curves were generated by taking the differences between the N(E) curves for the C and I phases (i.e. I-xC, when C and I are normalized to equal areas). Thus the "x" factors in Figs. 4 and 5 are not necessarily equal; however, curves similar to those in Fig. 5 could be obtained by simply integrating those in Fig. 4. The

difference curves in Fig. 5 have been normalized to equalize peak heights.

A comparison of the 1-xC curves with a self-fold of Feibelman's theoretical DOS, which reflects only C-M bonding, is shown in Fig. 5. The exact method for generating this self-fold will be described in Sec. 5. Features in the DOS self-fold generally align with those in the difference curves, and have similar intensities as well, particularly for the case when x = 0.8. This strongly suggests that the difference curves indeed reflect primarily C-M bonding character. On the other hand, features in the full 500K spectrum (curve a) do not align with the DOS self-fold, and do not have the same relative intensities. We believe the full 500K spectrum, and indeed all of the spectra in Fig. 3, contain additional contributions at higher binding energy due to the C-C bonding character.

5. Interpretation of Auger Spectra - Theoretical

We have quantitatively interpreted the carbidic lineshapes based on the ideas indicated above. The results are shown in Figs. 6, 7, and 8, and the relative intensities of the components are given in Table 2. The theoretical lineshape is generated by a least squares fit of three components to the experimental lineshape. The three components consist of 1) the C-M DOS self-fold, 2) the cross-fold of the C-C and C-M DOS, and 3) the C-C DOS self-fold; that is

$$N(E) = A\ \rho_{C\text{-}M} * \rho_{C\text{-}M} + B\ \rho_{C\text{-}M} * \rho_{C\text{-}C} + C\ \rho_{C\text{-}C} * \rho_{C\text{-}C}. \quad (1)$$

where $\rho * \rho$ indicates,

$$\rho * \rho(E) = (1-P_{ss}) \int \rho(E-\varepsilon)\rho(\varepsilon)d\varepsilon + P_{ss} \int \rho(14+E-\varepsilon)\rho(\varepsilon)d\varepsilon \quad (2)$$

The coefficients A, B, and C are determined by the least squares fit. As indicated in Sec. 4a above, no correlation effects are expected in the relatively unstable Ni_3C, so that these self-folds, modulated by the appropriate atomic Auger matrix elements

$$\rho * \rho = P_{kss}\ \rho_s * \rho_s + 2\ P_{ksp}\ \rho_s * \rho_p + P_{kpp}\ \rho_p * \rho_p, \quad (3)$$

are sufficient. Here P_{kss}:P_{ksp}:P_{kpp} were taken to be 0.8: 0.5: 1.0 consistent with that used previously [47,48].

The second term on the right in eq. (2) above is to account for the initial state shake-Auger (i.e. the kv-vvv) contribution, which accompanies the normal kvv Auger contribution. Upon creation of the initial core hole, there is a probability that a valence electron will leave with the core electron as a result of the dynamic screening process [49]. When the Auger decay occurs in the presence of this valence hole, this leaves 3 holes localized on a single carbon atom, resulting in a shift of the satellite relative to the main contribution. This kv-vvv contribution has been seen for several of the gas phase hydrocarbons [49], and for molecular and fragmented ethylene chemisorbed on Ni(100) at various temperatures [29].

For π-bonded ethylene/Ni at 100K, the relative satellite shift was found to be about 14 eV [29]; in the gas phase the shift is approximately 18 eV [41]. This difference reflects screening by the substrate electrons. 14 eV also gave the best fits for the carbidic lineshapes.

The probability for shakeoff (P_{ss})has been estimated to be about 0.2 for a free C atom [48,49], and we have found this value to be best also for the hydrocarbons [47], and for π-bonded ethylene/Ni [29]. However, one might expect that as the bond with the metal substrate becomes more intimate, that the probability for escape of this shake-hole before Auger decay might increase, thus decreasing the relative intensity, P_{ss}, of the shakeoff-Auger contribution. In this work we have tested the quality of the least squares fits with P_{ss} in eq. 2 set at 0.1, 0.15, and 0.2. Inclusion of the kv-vvv contribution clearly improves the agreement of theory with experiment, indicating that some kv-vvv contributions are present in the carbidic lineshapes, but the difference between the quality of the fits is not

sufficiently dramatic to determine the exact magnitude of P_{ss}. However, it lies somewhere between 0.15 and 0.2. We report the results for P_{ss} = 0.15 in Figs. 6-8, and for 0.1, 0.15, and 0.2 in Table 1. The effect of varying the shakeoff contribution is most dramatic on the C-C*C-C component, as expected since its intensity is largest where the shakeoff contribution is also large. Generally, the variation in the component intensity with the change in percent shakeoff gives an indication of the uncertainty in the results in Table 1.

The DOS representing the C-M bonding is obtained from the theoretical results of Feibelman [31] given in Fig. 1. To be more consistent with the empirical results, as reported in Fig. 1, we have shifted the "s" peak from 11 eV to 13 eV. We find, however, that the entire C-M self-fold, $\rho_{C-M}*\rho_{C-M}$, must be shifted by 2 eV to lower binding energy to provide an optimal fit to experiment, eq. 1. This is consistent with the observed shift of the large p_{xy} features seen in the Koel UPS data compared with the Feibelman result. Thus effectively the p_{xy} and p_z DOS of Feibelman are shifted by 1 eV to lower binding energy; the "s" feature by 1 eV to higher binding energy.

The calculations of Feibelman [31] suggest a ground state electronic configuration per C atom of $s^2p_{xy}^{1.75}p_z^{0.91}$, or a charge transfer of 0.66 electrons from the metal to the carbon. In contrast, the calculations of Joyner et al [26] suggest little charge transfer. However, with the non-self consistent cluster method and problems with the Wigner-Seitz radii used by Joyner et al, charge transfer is difficult to determine [26]. Below, we will use the results of Feibelman to normalize the s and p DOS. In the presence of a core hole, we expect an additional electron transfer to make the electronic configuration $s^2p_{xy}^{2.75}p_z^{0.91}$. Since the Final State Rule [50] indicates that the Auger lineshape should reflect the electronic charge configuration appropriate to the core hole state, we have normalized the calculated s and p DOS to reflect this electronic configuration.

The DOS representing the C-C bonding is more difficult to obtain. UPS data for ethylene on Ni(100) at 98 K shows the C-C π and σ bonding features at 4.7 and 8.4 eV respectively [14]. Upon heating the 4.7 eV feature moves to 4 eV, the 8.4 eV remains fixed [14]. Thus the C-C bonding may also have some DOS in the region where the C-M bonding contributes. However, such a contribution may not be important in interpreting the Auger lineshapes. Reported calculations on the C KVV lineshape in neopentane [51], a molecule containing 4 methyl groups surrounding a central carbon atom, indicate that the DOS self-fold for the methyl carbons is virtually identical to that for the central carbon. Our previous work on the C KVV Auger lineshape for the H-terminated diamond surface indicated similar results [52]. Thus as mentioned in Sec. 1. above, the C-C bonds are indistinguishable from C-H bonds in an Auger lineshape, and nearly so in UPS data. Demuth [30] has shown that C-H bonds in CH/metals produces a feature around 7-8 eV. This allows us to approximate the C-C DOS by utilizing the C-H DOS appropriate for methane. Methane has simple s and p features at 18 and 9 eV respectively [47]. The p feature reproduces the relatively narrow 8.4 eV feature seen by Koel [14]. The s feature is beyond the reported range of the UPS data given by Koel, but we believe evidence does exist for the C-H s*s feature in the Auger lineshapes in Fig. 6-8.

Figs. 6-8 show the results of the least squares fit of eq. 2 to the experimental data. These figures give direct evidence that the amount of C-C and C-M bonding character is reflected in the Auger lineshape. The C-M DOS self-fold gives peaks at 32, 22, 13 eV (these are the ss, sp and pp features) compared with 45, 36, and 27 eV for the C-C self-fold. This places the pp feature of the C-C self-fold at about the energy of the sp feature of the C-M self-fold. In fact, the principal peak in the experimental spectra appear to arise mostly from the pp feature of the C-C*C-M cross-fold. The larger so

called ss and sp features in the experimental surface carbidic lineshapes compared with the "bulk" carbides apparently result from the ss and sp components of the C-M$C-C cross-fold and sp and pp components of the C-C self-fold. The distinct high energy feature in the carbidic lineshapes appear to result from the pp feature in the C-M self-fold. The fact that each of the three components in eq. 2 account primarily for a different feature in the experimental spectra, decreases the linear dependence in the least squares fit, and allows for a more quantitative determination of the relative amounts of C-M and C-C bonding character in each case.

The agreement between the experimental spectra and the theoretical fits is generally very good, particularly in the important region between 15 and 38 eV. The larger differences beyond 40 eV arise from two sources. First, relatively large uncertainties exists beyond 40 eV in the experimental spectra because of uncertainties in removing the large extrinsic loss and background contributions in this region [53]. Second, as a general rule, the "ss" features in the Auger lineshape are very broad due to the vibrational manifold and the Franck-Condon principle [54]. This large broadening may not be adequately included in our empirical DOS self-folds.

The very large differences seen between 5 and 15 eV are believed to arise from a more fundamental phenomenon. The C-M DOS as reported by Feibelman (Fig. 1) has contributions from the non-bonding p_z, and the bonding p_{xy} and s orbitals. However, the non-bonding p_z orbitals become involved in the C-C bonds, as suggested by our interpretation of the EELS data in Sec. 3. This causes the p_z orbitals to become part of the C-C DOS. Obviously a fraction of the p_{xy} and s orbitals are also involved in C-C bonding, but not to the same extent. Therefore for self-consistency, a fraction of the $p_z$$p_z$, $p_z$$s$, and $p_z$$p_{xy}$ contributions in the C-M DOS self-fold should have been eliminated. This fraction should be equal to the fraction of

C atoms involved in C-C bonds, but of course this fraction is not known until after the least squares fit. Since the larger $p_z$$p_z$ and $p_z$$p_{xy}$ contributions fall in the 5-15 eV region, we made no attempt to eliminate them, but in anticipation of this effect, performed the least squares fit utilizing only the 15-40 eV region. The resultant large over-estimate of the Auger intensity between 5-15 eV provides evidence that the p_z orbitals are indeed involved in the C-C bonding, and support our interpretation of the EELS data.

The relative intensities of the 3 components for each of the fits is given in Table 1. Also shown are the relative component intensities expected for various C-C/C-M ratios. Comparison of these indicates that the C-C/C-M ratio is around 0.3 for C_2H_4/Ni(100), 0.5 for CO/Ni(100), and 0.35 for CO/Ni(111). This sequence is consistent with the relative heights of the shoulder at 15 eV, but inconsistent with the sharpness and apparent intensity of the peaks at 30 and 40 eV. This suggests that the 15 eV shoulder is the best qualitative indicator of C-C/C-M character. The 30 and 40 eV peaks have contributions from all three components, and Fig. 6-8 suggests their sharpness and intensity can change dramatically and non-uniformly with changes in C-C/C-M character. If one assumes that the C-C character increases with total carbon coverage, the estimated C-C/C-M ratios suggest that the total carbon coverages are considerably larger than the rough estimates of Houston (i.e. 0.1-0.2 ML on his Ni(100) and Ni(111) surfaces) or smaller than that given by Koel (0.19 ML on his Ni(100)).

We have not attempted to quantitatively interpret the low resolution curves a-c in Fig. 3. The shoulders at 15 eV in these broadened spectra are much less visible, but it is clearly present, particularly in curve c. We expect that the C-M/C-C ratio is not dramatically different from that for curve d, since they all are similar to this curve. For the bulk spectra, one might anticipate significant amounts of C-C character on the surface, but the carbide

layers underneath should consist primarily of C-M bonding and also contribute to the Auger spectra. Therefore, the bulk spectra are also expected to exhibit significant amounts of both C-C and C-M bonding.

6. Summary and Conclusions

A detailed interpretation of UPS, C K EELS, and C KVV Auger data has provided direct spectroscopic evidence for significant amounts of C-C bonding at the surface in addition to the C-M bonding with the substrate. The C-C bonding can arise from C_2, C_3 or higher polymer fragments on the surface. Our interpretation of the ELS and AES data on Ni(100) and Cu(100) then suggests that the C_x fragments breakup in the temperature range 570-670K below the temperature for formation of graphite.

The breakup of the C-C bonds on Ni and Cu (100) is consistent with trends seen in the data for ethylene fragmentation on transition metals. On Ru(001), negative ion SIMS studies [10] utilizing isotopic $C^{13}{}_2H_4$ and $C^{12}{}_2H_4$ mixtures show that the bonds (or least the association) between the two carbon atoms of the parent molecule remain up to 600K. However, above 600K, essentially complete carbon mobility exists, as suggested by the C^{13}-C^{13}, C^{13}-C^{12}, and C^{12}-C^{12} ion ratios (1:2:1) coming off the surface. This strongly suggests the breakup of the C-C bonds above 600K. In agreement with this data, Henderson et al [6] found that ethylene/Ru decomposes initially to CCH_3 (ethylidyne) which then decomposes via C-C bond cleavage. However, co-adsorption of CO and ethylene on Ru(001) causes the CCH_3 to decompose at higher temperatures to C_2H (acetylide), which then polymerizes ultimately to graphite without C-C bond cleavage. Henderson et al [6] conclude that the stabilization of CCH_3 by the CO on Ru mainly results from inhibition of C-C bond cleavage.

Generally, ethylene decomposes via two routes on transition metals. The first route initially involves acetylenic species (CCH, C_2H_2, and others), which typically occurs on the first row transition metal series, such as Ni(111), Fe(111), etc [6,9]. Although vinyl is the first decomposition fragment on Ni(100), we include Ni(100) in this group. The second route initially involves CCH_3 (ethylidyne), which typically occurs on Pt(111), Rh(111), Pd(111) etc [6,9]. The stabilization of ethylidyne apparently also results from inhibition of C-C bond cleavage on these latter metals. Thus Zhou et al [11] conclude that on Ni the C-C bonds tend to break more easily than the C-H bonds, while on Rh(111) and Pt(111), etc. the reverse is true. Consistently, they find on Pt(111), that C_2 units polymerize directly to graphite. Our finding that on Ni and Cu (100) the C-C bonds break around 600K before graphitization is also consistent with this picture.

The breaking of many of the C-C bonds on Ni and Cu in the 570-670 K range would suggest that the reactivity of the carbon layers would increase in this temperature range. This is of significant interest for Fischer-Tropsch synthesis, and for controlling the amounts of CH_4 and C_2H_6 produced in the process [22]. It also suggests that the graphite formation process involves C atom polymeriation on Ni and Cu. After more of the C-C bonds are broken, the C atoms may become more mobile, enabling the necessary adjustments in bond length and orbital structure required for formation of the graphitic islands and ultimately the graphite overlayer on these metals.

TABLE I. Component percentages as obtained from Eq. (2).

System	% shakeoff	Component percentages C-M‡C-M	C-M‡C-C	C-C‡C-C
C_2H_4/Ni(100)	10	63	31	6
600K	15	60	37	3
	20	60	31	9
CO/Ni(100)	10	42	45	12
500K	15	43	47	10
	20	47	42	10
CO/Ni(111)	10	55	33	12
500K	15	53	37	9
	20	68	30	2
Theory				
C-C/C-M = x		N*	N2x*	Nx^{2*}
0.20		69	28	3
0.25		64	32	4
0.30		59	36	5
0.35		55	38	7
0.40		51	41	8
0.50		44	44	11

*N = $100/(x^2 + 2x + 1)$

References

1. E.M. Stuve, R.J. Madix, and C.R. Brundle, Surf. Sci. 152/153 (1985) 532 .
2. M.M. Hills, J.E. Parmeter, and W.H. Weinberg, J. Am. Chem. Soc. 109 (1987) 4224 .
3. W. Erley, A.M. Baro, and H. Ibach, Surf. Sci. 120 (1982) 273.
4. S. Lehwald and H. Ibach, Surf. Sci. 89 (1979) 425.
5. J.E. Demuth and H. Ibach, Surf. Sci. 78 (1978) L238.
6. M.A. Henderson, G.E. Mitchell, and J.M. White, Surf. Sci. 203 (1988) 378.
7. F. Zaera and R.B. Hall, Surf. Sci. 180, 1 (1987).
8. F. Zaera and R.B. Hall, Surf. Sci. 180 (1987) 1.
9. A.M. Baro and H. Ibach, J. Chem. Phys. 74 (1981) 4194.
10. L.L. Lauderback and W.N. Delgass, Surf. Sci. 172 (1986) 715.
11. H.L. Zhou, X.Y. Zhu, and J.M. White, Surf. Sci. 193 (1988) 387.
12 X.Y. Zhu, M.E. Castro, S. Akhter, J.M. White, and J.E. Houston, Surf. Sci. 207 (1988) 1.
13. S. Akhter and J.M. White, Surf. Sci. 180 (1987) 19.
14. B.E. Koel, J.M. White, D.W. Goodman, Chem. Phys. Lett. 88 (1982) 236.
15. R. Rosei, S. Modesti, F. Sette, C. Quaresima, A. Savoia, and P. Perfetti, Phys. Rev. B29 (1984) 3416.
16. P. Tiscione and G. Rovida, Surf. Sci. 154 (1985) L255.
17. L.S. Caputi, G. Chiarello, and L. Papagno, Surf. Sci. 162 (1985) 259.
18. S. Santoni and J. Urban, Surf. Sci. 186 (1987) 376.
19. G. Chiarello, J. Andzelm, R. Fournier, N. Russo, and D.R. Salahub, 202 (1988) L621.

20. H. haarmann, B. Leidenberger, H. Hoinkes, and H. Wisch, Springer Series in Chemical Physics 14 (1982) 411.

21. F. Zaera, D.A. Fischer, R.G. Carr, J.L. Gland, J. Chem. Phys. 89 (1988) 5335.

22. D.W. Goodman, R.D. Kelly, T.E. Madey, and J.T. Yates, Jr., J. Catalysis 63 (1980) 226.

23. J.E. Houston, D.E. Peebles, and D.W. Goodman, J. Vac. Sci. Technol. A1 (1983) 995.

24. B.E. Koel and D.L. Neiman, Chem. Phys. Lett. 130 (1986) 164; B.E. Koel, private communication.

25. L. Papagno, L.S. Caputi, F. Ciccacci, and C. Mariani, Surf. Sci 128 (1383) L209.

26 R.W. Joyner, G.R. Darling, and J.B. Pendry, Surf. Sci. 205 (1988) 513.

27. J.W. Rabalais and S. Kasi, Science 239 (1988) 623.

28. D. Arvanitis, L. Wenzel, and K. Baberschke, Phys. Rev. Letters 59 (1987) 2435.

29. F.L. Hutson, D.E. Ramaker, B.E> Koel, S. Gebhard. submitted to Surf. Sci.

30. J.E. Dumuth, Surf. Sci. 69 (1977) 365; 93 (1980) 127.

31. P.J. Feibelman, Phys. Rev. B26, 5347 (1982); F.J. Himpsel, K. Christmann, P. Heimann, and D.E. Eastman, P.J. Feibelman, Surf. Sci. 115, L159 (1982).

32. J.H. Onuferko, D.P. Woodruff, and B.W. Holland. Surf. Sci. 87 (1079) 357.

33. J.E. Houston, J.W. Rogers, R.R. Rye, F.L. Hutson, and D.E. Ramaker, Phys. Rev. B34 (1986) 1215.

34. P.M.Th.M. van Attekum and G.K. Wertheim, Phys. Rev. Letter 43 (1979) 1896.

35. J.M. Schulga and G.L. Gutsev, J. Electron. Spectrosc. Related Phenom. 34 (1984) 39; Phys. Stat. Sol. 129 (1985) 683; 121 (1984) 595.

36. P.E. Pehrsson and D.E. Ramaker, J. Vac. Sci. Technol. A3 (1985) 1315; and to be published.

37. G.R. Gruzalski, D.M. Zehner, and G.W. Ownby, Surf. Sci. Lett. 157 (1985) L395.

38. A.K. Galwey, J. Catalysis 1 (1962) 227.

39. J.P. Coad and J.C. Riviere, Surf. Sci. 25, 609 (1971).

40. M.A. Smith and L.L. Levenson, Phys. Rev. B16 (1977) 1365.

41. S. Sinharoy, M.A. Smith, and L.L. Levenson, Surf. Sci. 72 (1978) 710; J. Vac. Sci. Technol. 14 (1977) 475.

42. J. Klefeld and L.L. Levenson, Thin Solid Films 64, 389 (1979).

43. C.C. Chang, "Analytical Auger Electron Spectroscopy, Characterization of Solid Surfaces" (P.F. Kane and G.B. Larrabee, Eds.), Plenum Press, New York, 1974.

44. M. Salmeron and A.M. Baro, Surf. Sci. 49 (1975) 356; M. Salmeron, A.M. Baro, and J.M. Rojo, Phys. Rev. B13 (1976) 4348.

45. D.A. Shirley, Phys. Rev. B5, 4707 (1972).

46. R.R. Rye, T.E. Madey, J.E. Houston, and P.H. Holloway, J. Chem. Phys. 69 (1979) 1504; Ind. Eng. Chem. Prod. Res. Dev. 18 (1979) 2; R.R. Rye, D.R. Jennison, and J.E. Houston, J. Chem. Phys. 73 (1980) 4867.

47. F.L. Hutson and D.E. Ramaker, J. Chem. Phys. 87 (1987) 6824.

48. F.L. Hutson, D.E. Ramaker, B.I. Dunlap, J.D. Ganjei, and J.S. Murday, J. Chem. Phys. 76 (1982) 2181.

49. T.A Carlson, C.W. Nestor, Jr., T.C. Tucker, and F.B. Malik, Phys. Rev. 169 (1968) 27.

50. F.L. Hutson and D.E. Ramaker, submitted to Surf. Sci.

51. F.L. Hutson and D.E. Ramaker, Phys. Rev. B35 (1987) 9799.

52. D.R. Jennison, J.A. Kelber, and R.R. Rye, Phys Rev. B25 (1982) 1384.

53. D.E. Ramaker and F.L. Hutson, Solid State Commun. 63 (1987) 335.

54. D.E. Ramaker, J.S. Murday, and N.H. Turner, J. Electron Spectrosc. Related Phenom. 17 (1970) 45.

55. B.I. Dunlap, P.A. Mills, and D.E. Ramaker, J. Chem. Phys. 75 (1981) 300.

FIGURE CAPTIONS

Fig. 1. Comparison of the C valence band DOS for carbidic carbon obtained from UPS difference curves for CO/Ni(111) at 500K (Rosei et al [15]) and C_2H_4/Ni(100) at 580 K (Koel et al [14]), and from LCAO-MO theoretical calculations for a (1x1) overlayer of C atoms on an 11-layer Ru(0001) film (Feibelman [31]). See text for details.

Fig. 2. Comparison of C K EELS data for CO on the Ni surfaces and temperatures indicated. The G, C, or I indicate the graphitic, carbidic, or intermediate phases, respectively. Curves a)-c) are from Caputi et al. [17] and curve d) from Rosei et al. [15].

Fig. 3. Comparison of C KVV Auger lineshapes for carbidic carbon, obtained from CO on the Ni surfaces and temperatures indicated. Curves a) and d)-f) are for surface carbidic carbon (i.e. less than 1 ML), curves b) and c) for films of "bulk-like" carbon. Curve a) is from Caputi et al [17], b) from Chang [43], c) from Salmeron et al [44], d) and e) from Houston et al [23], and f) from Koel [24]. See text for details on data treatment and energy alignment.

Fig. 4 Comparison of Auger data for CO/Ni(100) at 520 K and 620 K as reported by Caputi et al [17]. These represent the carbidic (C) and intermediate (I) phases, respectively. Also shown are difference curves, I-xC, with the weighting factor x indicated for equal peak-to-peak heights in I and C.

Fig. 5 Comparison of the full Auger lineshape for CO/Ni(100) at 520 K with difference curves, I-xC, with the weighting factor x indicated for normalized N(E) areas. Also shown is a self-fold of Feibelman's theoretical DOS obtained as described in the text (solid line), and a 1.75 eV Gaussian broadened self-fold (dashed line).

Fig. 6 Comparison of the experimental (Koel [24]) and theoretical (least squares fitted from eq. (2)) Auger lineshapes for C_2H_4/Ni(100). Also shown are the three components obtained as described in the text.

Fig. 7 Same as Fig. 6 but for CO/Ni(100) as obtained by Houston [23].

Fig. 8 Same as Fig. 6 but for CO/Ni(111) as obtained by Houston [23].

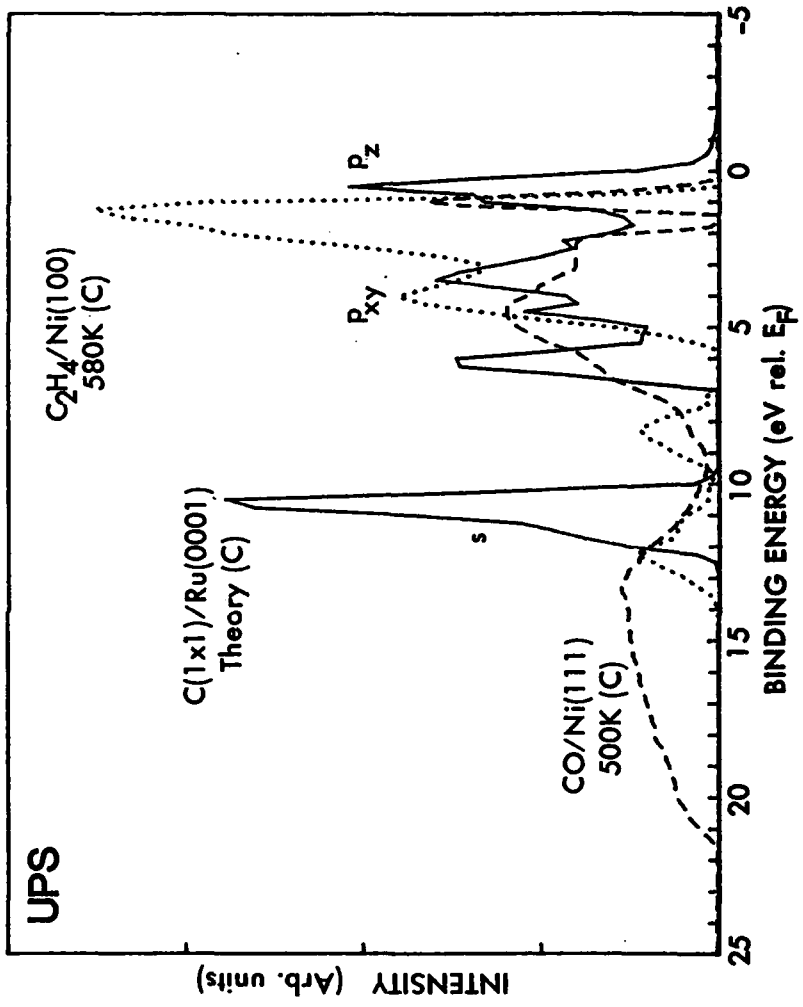

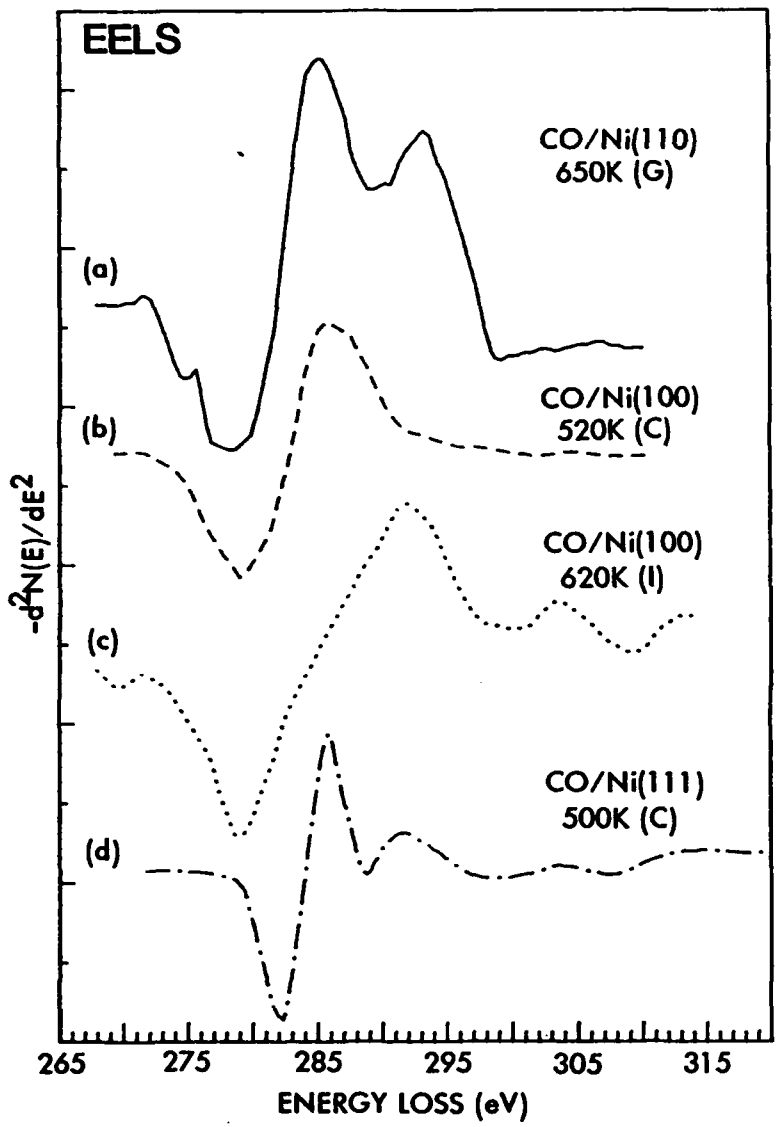
EELS
CO/Ni(110)
650K (G)
(a)
CO/Ni(100)
520K (C)
(b)
CO/Ni(100)
620K (I)
(c)
CO/Ni(111)
500K (C)
(d)
$-d^2N(E)/dE^2$
265
275
285
295
305
315
ENERGY LOSS (eV)

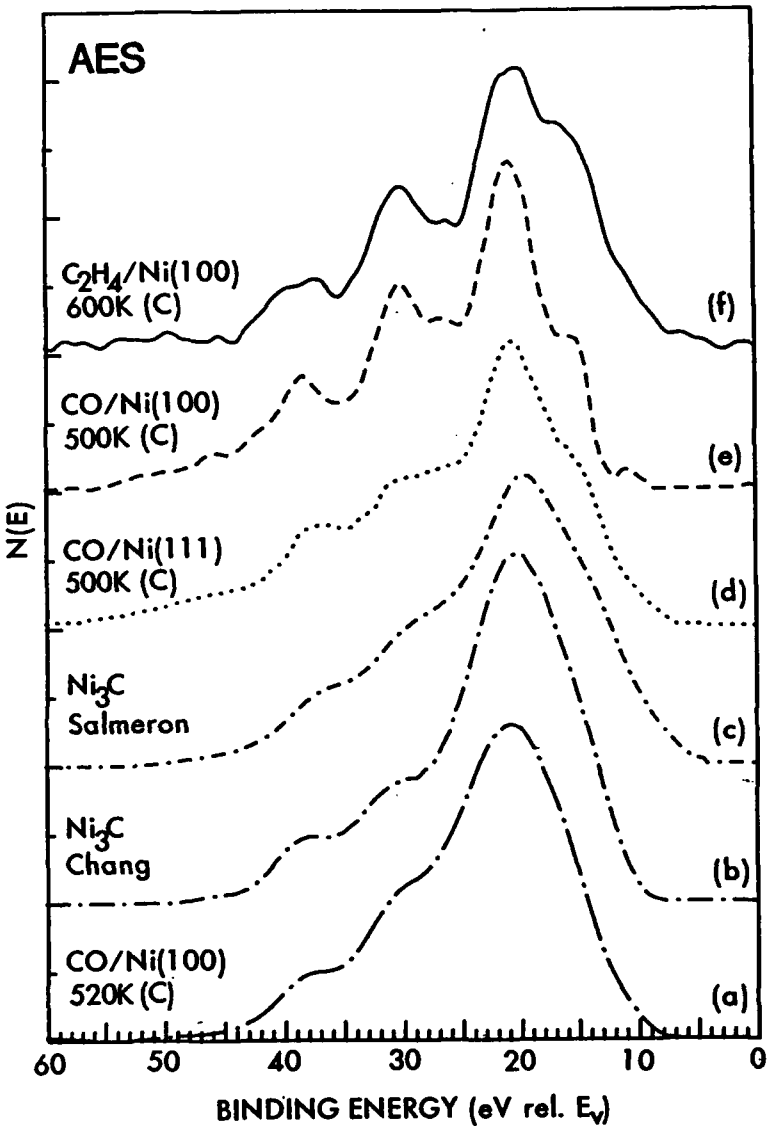
AES
C_2H_4/Ni(100)
600K (C)
(f)
CO/Ni(100)
500K (C)
(e)
CO/Ni(111)
500K (C)
(d)
Ni_3C
Salmeron
(c)
Ni_3C
Chang
(b)
CO/Ni(100)
520K (C)
(a)
N(E)
60
50
40
30
20
10
0
BINDING ENERGY (eV rel. E_v)

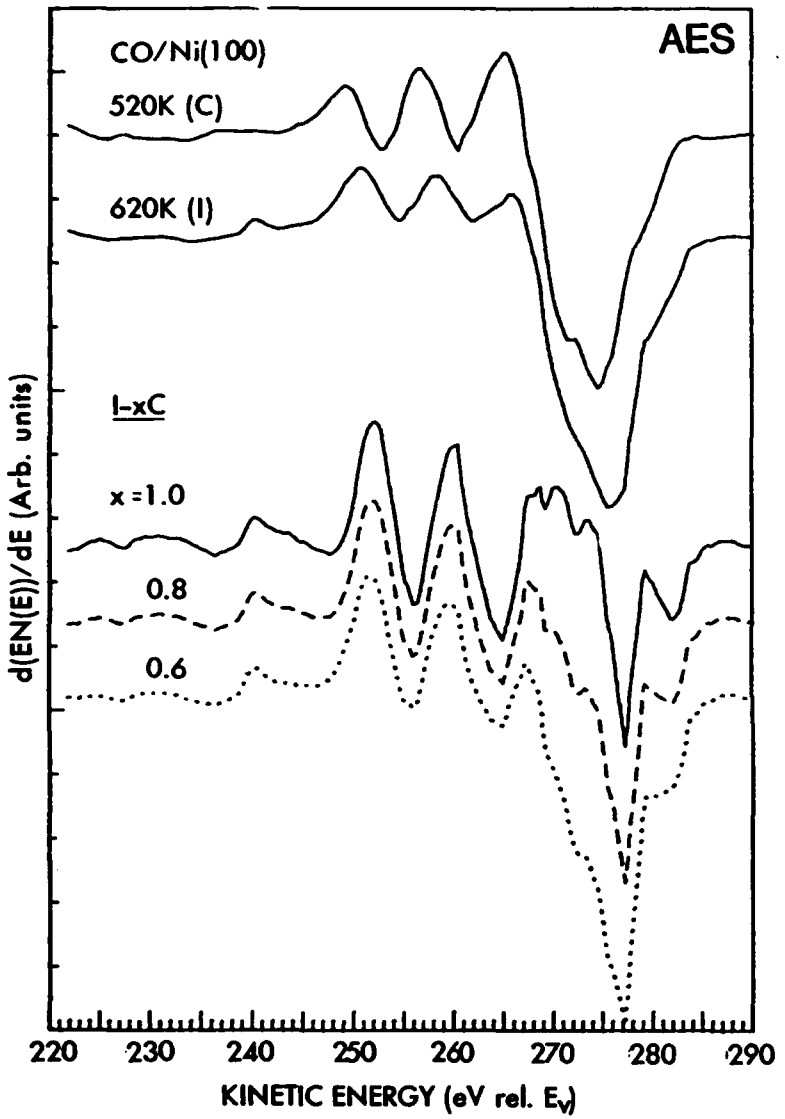
AES
CO/Ni(100)
520K (C)
620K (I)
I-xC
x=1.0
0.8
0.6
d(EN(E))/dE (Arb. units)
220
230
240
250
260
270
280
290
KINETIC ENERGY (eV rel. E_v)

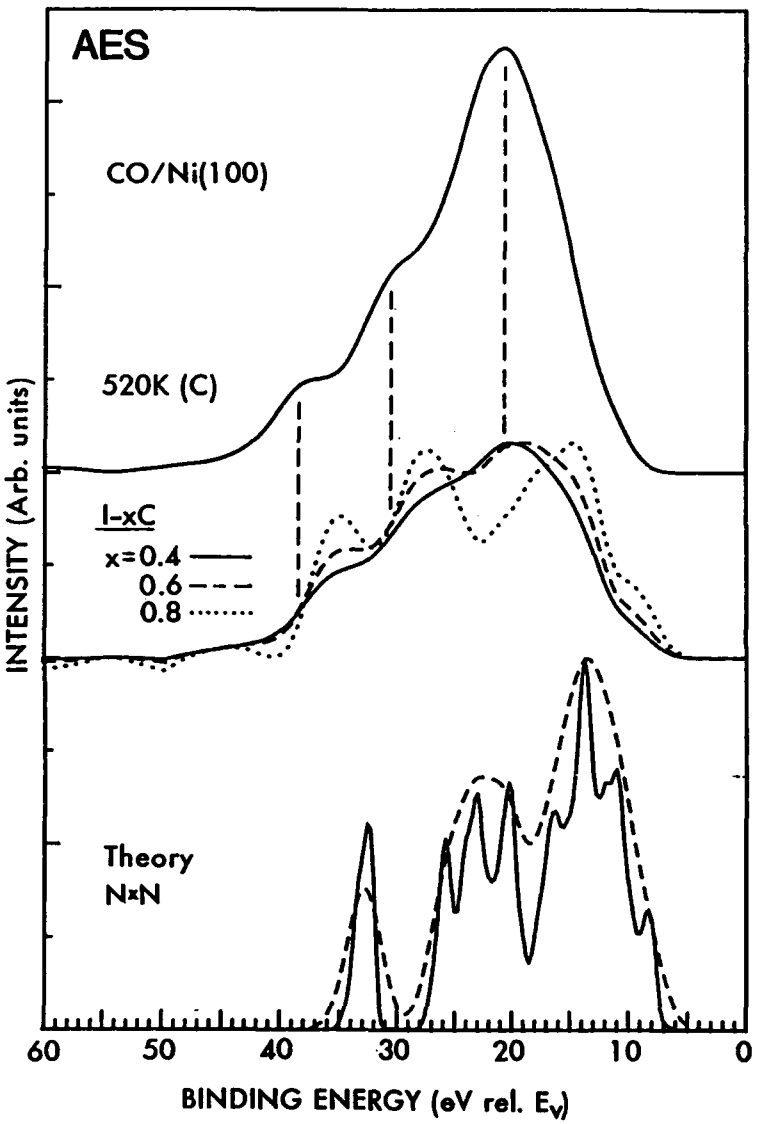
AES
CO/Ni(100)
520K (C)
I-xC
x=0.4
0.6
0.8
Theory
N×N
INTENSITY (Arb. units)
60
50
40
30
20
10
0
BINDING ENERGY (eV rel. E_v)

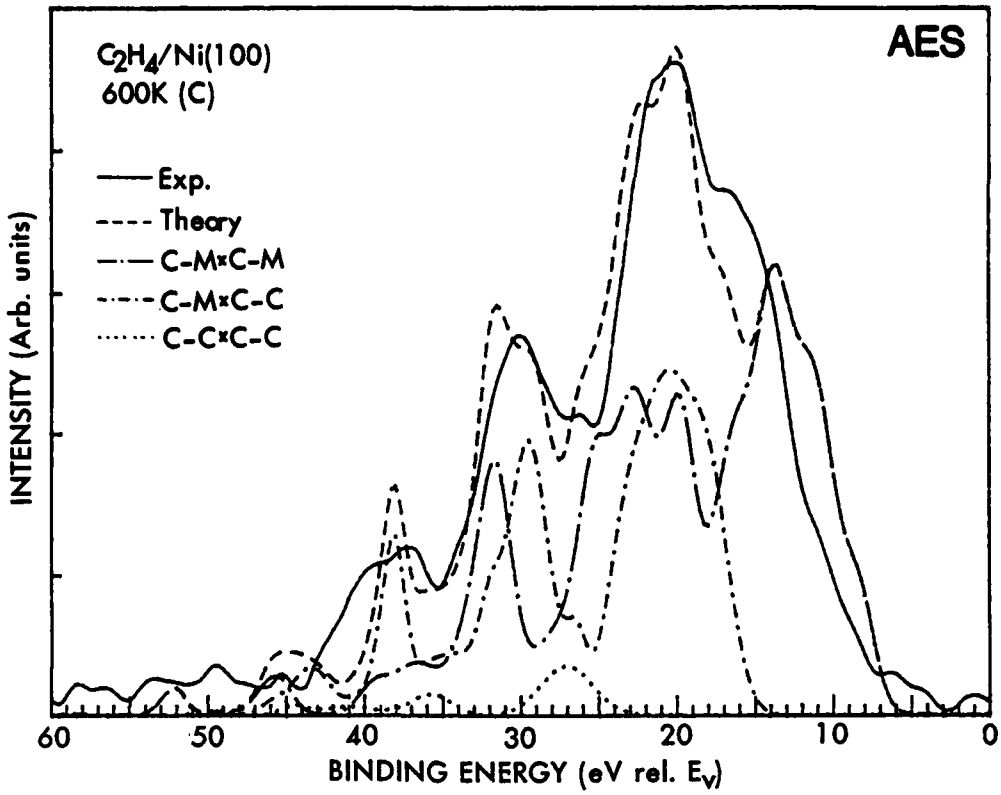
AES
C_2H_4/Ni(100)
600K (C)
Exp.
Theory
C-M×C-M
C-M×C-C
C-C×C-C
INTENSITY (Arb. units)
60
50
40
30
20
10
0
BINDING ENERGY (eV rel. E_V)

6.

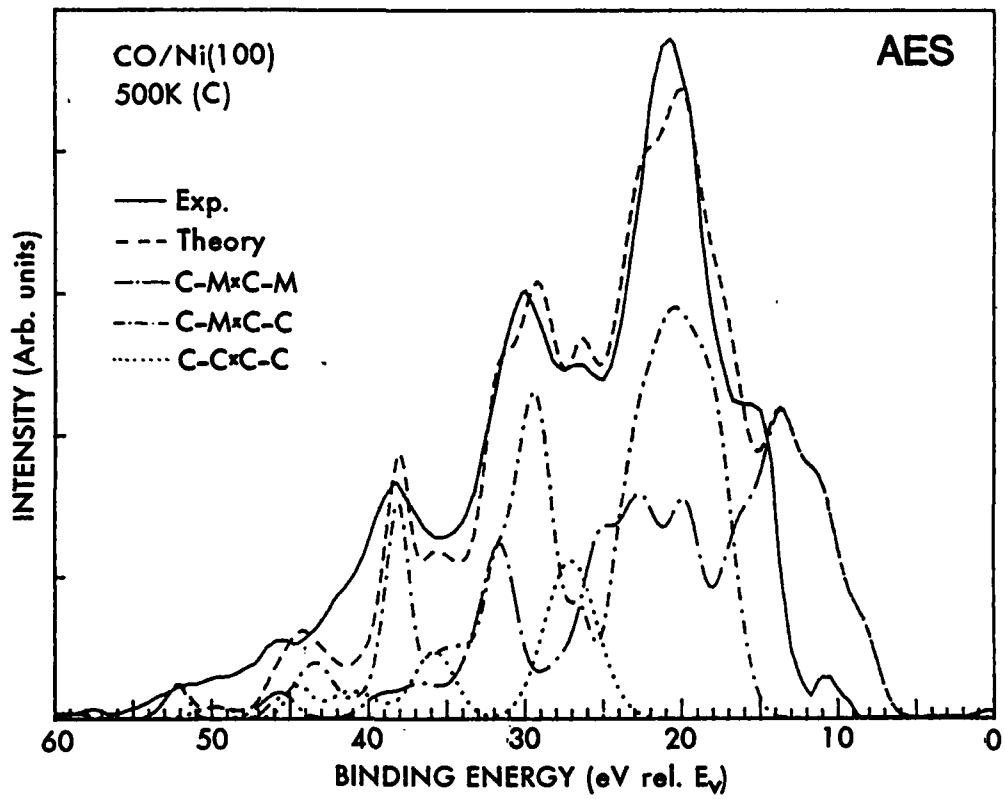
AES
CO/Ni(100)
500K (C)
Exp.
Theory
C-M×C-M
C-M×C-C
C-C×C-C
INTENSITY (Arb. units)
60
50
40
30
20
10
0
BINDING ENERGY (eV rel. E_V)

7

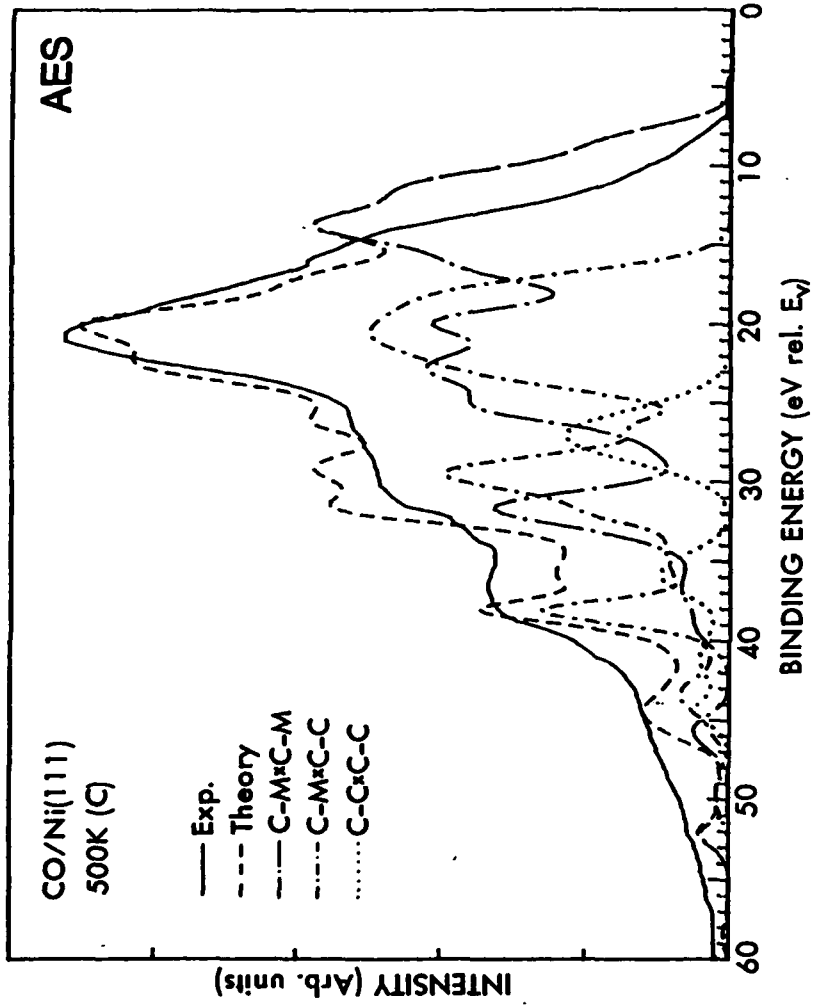

DL/1113/89/1

TECHNICAL REPORT DISTRIBUTION LIST, GENERAL

	No. Copies
Office of Naval Research Chemistry Division, Code 1113 800 North Quincy Street Arlington, VA 22217-5000	3
Commanding Officer Naval Weapons Support Center Attn: Dr. Bernard E. Douda Crane, IN 47522-5050	1
Dr. Richard W. Drisko Naval Civil Engineering Laboratory Code L52 Port Hueneme, California 93043	1
Defense Technical Information Center Building 5, Cameron Station Alexandria, Virginia 22314	2 high quality
David Taylor Research Center Dr. Eugene C. Fischer Annapolis, MD 21402-5067	1
Dr. James S. Murday Chemistry Division, Code 6100 Naval Research Laboratory Washington, D.C. 20375-5000	1
Dr. Ronald L. Atkins Chemistry Division (Code 385) Naval Weapons Center China Lake, CA 93555-6001	1
Chief of Naval Research Special Assistant for Marine Corps Matters Code 00MC 800 North Quincy Street Arlington, VA 22217-5000	1
Dr. Bernadette Kirchinger Naval Ship Systems Engineering Station Code 053 Philadelphia Naval Base Philadelphia, PA 19112	1
Dr. Sachio Yamamoto Naval Ocean Systems Center Code 52 San Diego, CA 92152-5000	1
David Taylor Research Center Dr. Harold H. Singerman Annapolis, MD 21402-5067 ATTN: Code 283	1